

**ISSN 1011-372X, Volume 136, Combined 1-2**



**This article was published in the above mentioned Springer issue.  
The material, including all portions thereof, is protected by copyright;  
all rights are held exclusively by Springer Science + Business Media.  
The material is for personal use only;  
commercial use is not permitted.  
Unauthorized reproduction, transfer and/or use  
may be a violation of criminal as well as civil law.**

# Influence of Indium Content on the Properties of Pt–Re/Al<sub>2</sub>O<sub>3</sub> Naphtha Reforming Catalysts

Viviana M. Benitez · Carlos L. Pieck

Received: 30 August 2009 / Accepted: 22 October 2009 / Published online: 5 November 2009  
© Springer Science+Business Media, LLC 2009

**Abstract** The influence of indium on the properties of Pt–Re/Al<sub>2</sub>O<sub>3</sub> catalysts used in naphtha reforming is studied. The addition of indium to the Pt–Re/Al<sub>2</sub>O<sub>3</sub> catalyst produces a big decrease of acidity. It also produces an inhibition of the metal function, i.e., dehydrogenation and hydrogenolysis activity. The reaction of n-C<sub>5</sub> isomerization shows that indium addition decreases the total activity of the Pt–Re catalyst but increases the selectivity to the i-C<sub>5</sub> isomers. The selectivity to low cost light gases (C<sub>1</sub>–C<sub>3</sub>) is particularly decreased. The reaction of n-C<sub>7</sub> reforming showed that addition of indium increases the stability of the catalyst and the selectivity to aromatics, and decreases the production of light gases.

**Keywords** Naphtha reforming · Trimetallic catalysts · Indium

## 1 Introduction

Catalytic reforming is a very important chemical process in the petrochemical industry. Both aromatic hydrocarbons (BTX) and high octane gasoline are produced in catalytic reformers. From a chemical point of view, the molecular structure of straight run naphtha hydrocarbons is reordered without significant changes in chain length. In this way branched chain isomers and cyclic hydrocarbons (naphthenes and aromatics) are formed from normal paraffins present in the naphtha feed. In order to promote the desired

reaction paths (i.e. isomerization, cyclization and aromatization) naphtha reforming catalysts must have both acid and metal functions. The metal function is usually supplied by dispersed Pt particles modified by so-called metal promoters. The acid function is supplied by the acidic support, usually chlorided gamma alumina.

Bimetallic Pt–Re/Al<sub>2</sub>O<sub>3</sub> catalysts were patented in 1968 [1] and found rapid acceptance in the refining industry. They had a higher selectivity and stability than the previous monometallic Pt/Al<sub>2</sub>O<sub>3</sub> catalysts and allowed the process to be carried out at lower pressures and for longer periods without regeneration. The associated benefits of lower operating cost boosted the interest of the industry and scientific laboratories to develop new catalysts with improved properties of activity, selectivity and stability. Several bimetallic catalysts were thus proposed for commercial use. Only a few made their road into commercial operation, such as Pt–Re, Pt–Sn, Pt–Ir and Pt–Ge catalysts.

The current trend in the manufacture of commercial catalysts is to produce catalysts with extended operation cycle. This is achieved by reducing the deactivation of the catalysts by coke deposition. Many patents propose the use of trimetallic catalysts [2, 3]. Some of them claim that these catalysts yield an improvement of the isoparaffins/aromatics ratio in the reformat product. This is deemed convenient for the compliance of environmental regulations that limit the content of aromatics and mainly benzene in motor gasolines [2, 3].

The activity, selectivity and stability of the catalysts for naphtha reforming not only depend on the metal components but also on their oxidation state, their degree of interaction (alloying) and the dispersion of the Pt particles. The nature of the catalyst surface also strongly depends on the method of preparation and the activation pretreatment of the metal function components.

V. M. Benitez · C. L. Pieck (✉)  
Instituto de Investigaciones en Catálisis y Petroquímica,  
INCAPE (FIQ-UNL, CONICET), Santiago del Estero 2654,  
3000 Santa Fe, Argentina  
e-mail: pieck@fiq.unl.edu.ar

To improve the efficiency of catalytic reforming catalysts some patents advocate the incorporation of In. Wilhelm [4] reports that the addition of indium markedly improves the activity, selectivity and stability. Antos [5] proposes the use of catalysts containing indium in order to obtain rich aromatic cuts that would be adequate for petrochemical use. They also report that the addition of indium improves the resistance to deactivation by coke formation. In agreement with them, Bogdan and Imai [3, 6] report that indium improves the aromatization/cracking ratio of the reforming reaction and increases the production of gasoline. More recently Peltier et al. [7] have proposed the use of various catalysts containing Pt and other metals (Re, In, Sn, W).

The objective of this work was to study the activity and deactivation characteristics of Pt–Re–In trimetallic catalysts for naphtha reforming.

## 2 Experimental

### 2.1 Catalysts Preparation

All catalysts were prepared using a commercial  $\gamma$ -alumina as support (Cyanamid Ketjen CK-300, pore volume =  $0.5 \text{ cm}^3/\text{g}$ , specific surface area =  $180 \text{ m}^2/\text{g}$ , impurities: Na = 5 ppm, Fe = 150 ppm, S = 50 ppm). The alumina pellets were ground to obtain grains of 177–500  $\mu\text{m}$  in diameter and afterwards calcined in air at  $650 \text{ }^\circ\text{C}$  for 3 h. Then 0.2 M HCl was added to the support and the slurry was left unstirred for 1 h at room temperature. Later,  $\text{H}_2\text{PtCl}_6$ ,  $\text{NH}_4\text{ReO}_4$  and  $\text{NO}_3\text{In}$  impregnating solutions were added to the system and the slurry was shaken gently for 1 h at room temperature. Then it was dried at  $70 \text{ }^\circ\text{C}$  until a dry solid was obtained. Drying was completed in an oven at  $120 \text{ }^\circ\text{C}$ . The concentration of the impregnating solutions was adjusted in order to obtain 0.3% Pt, 0.3% Re and 0.3 or 0.1% In on the final catalysts. Then the catalysts were activated by calcination in air at  $450 \text{ }^\circ\text{C}$  for 4 h and cooled down to room temperature in nitrogen. They were then reduced in hydrogen ( $60 \text{ cm}^3 \text{ min}^{-1}$ ) at  $500 \text{ }^\circ\text{C}$  for 4 h. Heating ramps were programmed at  $10 \text{ }^\circ\text{C min}^{-1}$ .

### 2.2 Temperature Programmed Reduction (TPR)

These tests were performed in an Ohkura TP2002 equipment provided with a thermal conductivity detector. At the beginning of each TPR test the catalyst samples were pretreated in situ by heating in air at  $250 \text{ }^\circ\text{C}$  for 1 h. Then they were heated from room temperature to  $700 \text{ }^\circ\text{C}$  at  $10 \text{ }^\circ\text{C min}^{-1}$  in a gas stream of 5.0% hydrogen in argon.

### 2.3 Temperature Programmed Desorption of Pyridine

The amount and strength of the acid sites of the catalysts were assessed by means of temperature programmed desorption of pyridine (Py). 200 mg of the catalyst to be tested were first immersed for 4 h in a closed vial containing pure pyridine (Merck (99.9%)). Then the vial was opened and excess base was allowed to evaporate in a ventilated hood at room conditions until the surface of the particles was dry. The sample was then loaded into a quartz tube microreactor and supported over a quartz wool plug. A constant flow of nitrogen ( $40 \text{ mL min}^{-1}$ ) was made to flow over the sample all throughout the experiment. A first step of desorption of weakly adsorbed base and stabilization was performed by heating the sample at  $110 \text{ }^\circ\text{C}$  for 2 h. Then the temperature of the oven was raised to a final value of  $500 \text{ }^\circ\text{C}$  at a heating rate of  $10 \text{ }^\circ\text{C min}^{-1}$ . The reactor outlet was directly connected to a flame ionization detector. The detector signal (in mV units) was sampled at 1 Hz and recorded in a computer device.

### 2.4 Cyclopentane Hydrogenolysis (HCP)

Before the reaction the catalysts were reduced for 1 h at  $500 \text{ }^\circ\text{C}$  in  $\text{H}_2$  ( $60 \text{ cm}^3 \text{ min}^{-1}$ ). Then they were cooled in  $\text{H}_2$  to the reaction temperature ( $350 \text{ }^\circ\text{C}$ ). The other conditions were: catalyst mass = 150 mg, pressure = 0.1 MPa,  $\text{H}_2$  flow rate =  $40 \text{ cm}^3 \text{ min}^{-1}$ , cyclopentane flow rate =  $0.483 \text{ cm}^3 \text{ h}^{-1}$  and molar ratio  $\text{H}_2:\text{CP} = 20$ . The reaction products were analyzed in a gas chromatograph connected on-line.

### 2.5 Cyclohexane Dehydrogenation (DCH)

The reaction was performed in a glass reactor with the following conditions: catalyst mass = 100 mg, temperature =  $300 \text{ }^\circ\text{C}$ , pressure = 0.1 MPa,  $\text{H}_2 = 80 \text{ cm}^3 \text{ min}^{-1}$ , cyclohexane =  $1.61 \text{ cm}^3 \text{ h}^{-1}$  and molar ratio  $\text{H}_2:\text{CH} = 14$ . Before the reaction was started the catalysts were treated in  $\text{H}_2$  ( $80 \text{ cm}^3 \text{ min}^{-1}$ ,  $500 \text{ }^\circ\text{C}$ , 1 h). The reaction products were analyzed in a gas chromatograph connected on-line.

### 2.6 *n*-Pentane Isomerization

The reaction was carried out for 4 h in a continuous flow glass reactor at atmospheric pressure,  $500 \text{ }^\circ\text{C}$ , WHSV = 4.5 and molar ratio  $\text{H}_2:n\text{-C}_5 = 6$ . *n*-C<sub>5</sub> was supplied by Merck (99.9%). The analysis of reactants and products was performed using a Varian 3400 CX gas chromatograph equipped with a flame ionization detector. A packed column of dimethyl sulfolane on Chromosorb P (ID 1/8" in, 3 m length) maintained at  $40 \text{ }^\circ\text{C}$  was used for the chromatographic

separation of the products. The conversion of  $n\text{-C}_5$  was defined as:

$$n\text{-C}_5 \text{ conv.} = \frac{n - C_5^i - n - C_5^0}{n - C_5^i} \quad (1)$$

$n - C_5^i$  is the number of  $n\text{-C}_5$  molecules at the reactor inlet and  $n - C_5^0$  is the number at the reactor outlet. The selectivity to each product  $i$  was defined as:

$$S_i = \frac{\text{yield of } i}{n\text{-C}_5 \text{ conv.}} = \frac{A_i \cdot f_i \cdot n_i}{M_i \left( \sum \frac{A_i f_i n_i}{M_i} \right) n\text{-C}_5 \text{ conv.}} \times 100 \quad (2)$$

$A_i$  is the area of the chromatographic peak of product  $i$ ,  $f_i$  is its response factor,  $n_i$  is the number of carbon atoms of  $i$  and  $M_i$  is its molecular weight.

### 2.7 *n*-Heptane Reforming

The reaction was performed in a fixed bed tubular reactor under the following conditions: 0.1 MPa, 500 °C,  $\text{H}_2/n\text{-C}_7 = 6$ ,  $\text{WHSV} = 4 \text{ h}^{-1}$ . The catalysts were first reduced in  $\text{H}_2$  ( $12 \text{ cm}^3 \text{ min}^{-1}$ ) for 1 h at 500 °C. The analysis of the reaction products was made using a ZB-1 capillary column and a flame ionization detector. The conversion of  $n\text{-C}_7$  and the selectivity to each product was calculated using formulae similar to those defined for  $n\text{-C}_5$ .

### 2.8 Temperature-programmed Oxidation

Carbon deposits forming on the surface of the catalysts were studied by means of temperature-programmed oxidation (TPO). 40–60 mg of the coked catalyst were first charged in a quartz reactor. Then the carbon was burned in an oxidizing stream ( $60 \text{ cm}^3 \text{ min}^{-1}$  of diluted oxygen, 5%  $\text{O}_2$  in  $\text{N}_2$  vol:vol). The temperature of the cell was increased from 30 to 650 °C with a heating rate of  $10 \text{ °C min}^{-1}$ . The outlet gases were fed to a methanation reactor where  $\text{CO}_2$  and  $\text{CO}$  were quantitatively transformed into  $\text{CH}_4$  over a Ni catalyst in the presence of  $\text{H}_2$ . The  $\text{CH}_4$  stream was connected to a flame ionization detector (FID) and the signal produced was continuously recorded in a computer. The carbon concentration of the catalysts was calculated from the area of the TPO trace (FID signal as a function of the temperature of the cell) by reference to calibration experiments performed with catalysts with known carbon amounts.

The absence of mass transfer limitations was assessed by calculating the modulus of Weisz-Prater and the Damköhler number for all the reactions involved: CH dehydrogenation, CP hydrogenolysis, *n*-pentane isomerization and  $n\text{-C}_7$  reforming. In all cases the Weisz-Prater modulus was found to be much smaller than 0.1 while the Damköhler number was smaller than 0.01. Mass transfer

problems were thus disregarded. For the calculus, kinetic parameters were conservatively estimated from maximum initial reaction rate values by assuming first-order kinetics. Transport coefficients were estimated from known correlations.

## 3 Results and Discussion

Figure 1 shows the TPR traces of the  $\text{In}/\text{Al}_2\text{O}_3$  and  $\text{Pt-Re-In}(x)/\text{Al}_2\text{O}_3$  catalysts. Previous reported results [8, 9] indicate that the Pt has a large reduction peak at 240–260 °C attributed to the reduction of most of the Pt oxide and a small reduction peak at 300 °C corresponding to the reduction of oxychlorinated platinum species in strong interaction with alumina. Supported Re has a broad reduction peak centered at approximately 590 °C, with a small shoulder at low temperatures due to the reduction of species with a lower interaction with the support.

A reduction peak centered at ca. 360 °C was found in the case of the monometallic (0.35% In) catalyst (Fig. 1). Differences in the reduction profiles of supported indium oxides have been generally attributed to variations in oxide particle size. Smaller particles are reduced at lower temperatures [10, 11]. The bimetallic Pt–Re catalyst has three reduction peaks. The first one, centered at ca. 250 °C is due to the reduction of oxidized Pt species. The intermediate band (ca. 350 °C) corresponds to the Pt-catalyzed reduction of rhenium oxides. The high temperature (ca. 550 °C) peak could be attributed to the reduction of segregated rhenium oxides. On the other hand, the bimetallic Pt–In (0.3% Pt, 0.3% In) catalyst exhibits two reduction peaks,

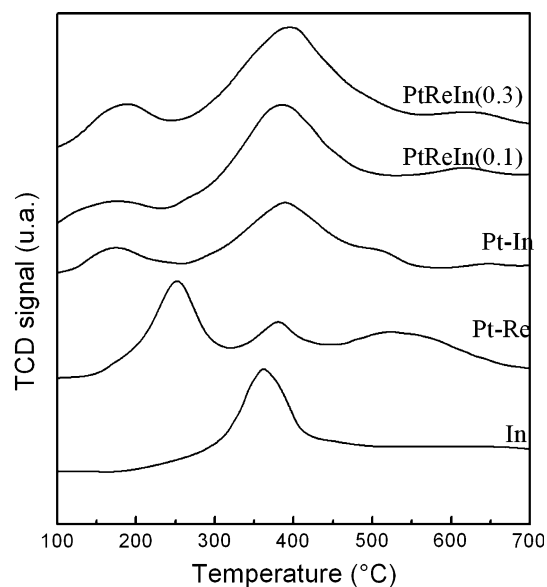


Fig. 1 TPR traces of the studied catalysts

centered at 150 and 390 °C respectively. The lower temperature peak could be due to the reduction of Pt species weakly interacting with indium while the higher temperature peak could be attributed to Pt species strongly modified by the presence of In.

The results indicate that indium interacts with Pt and modifies its reducing pattern. The lower reduction temperature (peak at 150 °C) would be the result of a decreased Pt-support interaction induced by indium. In the case of the trimetallic catalysts the addition of indium to Pt-Re increases the size of the peak at 390 °C. For this reason this peak could be due to the reduction of In and Re species in close interaction with Pt. The shoulder at 590 °C corresponds to segregated Re species.

The measurement of the amount of base evacuated as a function of programmed heating temperature gives a measure of the acid strength distribution while the area below the TPD curves is proportional to the total acid sites [12–14]. It can be seen in Fig. 2 that the total acidity is decreased by indium addition. These results are in agreement with previously published reports [15] that indicate that in spite of indium being an amphoteric oxide its surface oxidized species are slightly basic. When deposited over the acid sites of the support, oxidized indium species would block some of these sites and hence would cause a decrease of the total acidity. Another factor contributing to decrease the acidity by addition of indium is the displacement of Cl atoms from Al sites where they generate acidity to other sites where they behave as spectators.

The properties of the metal function were assessed by means of the test reactions of cyclopentane hydrogenolysis (HCP) and cyclohexane dehydrogenation (DCH). Table 1

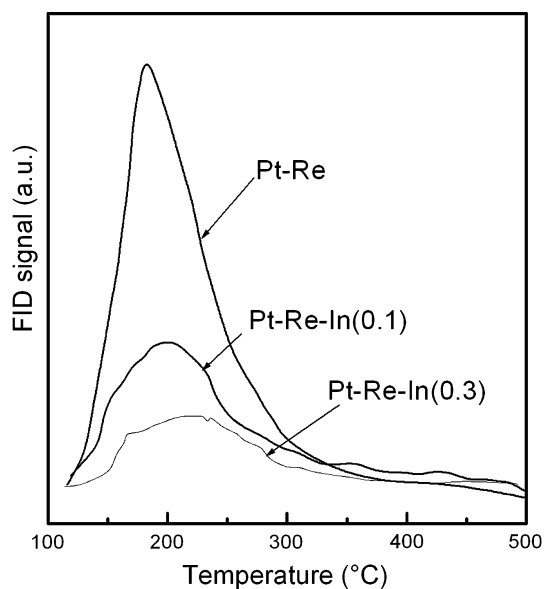


Fig. 2 Pyridine TPD traces of the studied catalysts

**Table 1** Values of conversion obtained in the reactions of cyclopentane (CP) hydrogenolysis and cyclohexane (CH) dehydrogenation

Catalysts	Conversion of CP (%)	Conversion of CH (%)
Pt <sup>a</sup>	27.6	56.0
Pt-Re	42.0	47.6
Pt-Re-In(0.1)	8.9	37.7
Pt-Re-In(0.3)	4.5	34.1

<sup>a</sup> Pieck et al. [16]

contains values of conversion of cyclopentane at 5 min time-on-stream and average values of conversion of cyclohexane. The hydrogenolytic activity decays rapidly due to the formation and accumulation of coke. Conversely the cyclohexane dehydrogenation is not affected by deactivation and it is also 100% selective to the formation of benzene. It can be seen that the Pt catalyst is more active in CH dehydrogenation than the Pt-Re catalyst. The opposite occurs in the CP hydrogenolysis reaction. These results were previously explained considering the different sites involved in each reaction [16]. In the case of the hydrogenolysis reaction the active sites are ensembles of Pt-Re while for the hydrogenation reaction the activity is due to Pt atoms. The results of Table 1 indicate that addition of indium produces a blocking of the sites with hydrogenolytic capacity. This is reflected by the acute drop in the conversion of cyclopentane. The inhibition can be explained by recalling that the reaction of hydrogenolysis begins with the adsorption of two neighbouring carbon atoms over adjacent metal sites. Then the C-H bonds are cleaved. The carbon atoms continue to be dehydrogenated, thus increasing the strength of their bond to the metal and decreasing the strength of the C-C bond. The strength of the metal-carbon bond is crucial for the progress of the reaction. The metal-carbon bond is difficult to form and requires the presence of a pair of neighbouring metal atoms or better, of an ensemble of them. It can be verified that hydrogenolysis needs of an ensemble of atoms of minimum size to proceed. For this reason is considered a demanding reaction [17]. The loss of activity of the indium doped catalysts in the HCP reaction can then be attributed to a reduction of the size of the Pt-Re ensembles. This size reduction is caused by the intercalation of indium atoms in the metal function. On the other side, the DCH reaction is called a non-demanding reaction (easy or structure-insensitive reaction) [18]. Therefore the inhibiting effect of indium is expected to be much greater for the HCP reaction than for the DCH one.

It is widely accepted that the isomerization of short paraffins occurs by a bifunctional metal-acid mechanism [19]. The reaction begins on the metal site with the dehydrogenation of the paraffin to an olefin. Then the olefin is

converted to an isomeric alkene over an acid site. This alkene is finally hydrogenated over a metal site and the final isoparaffin is formed. This reaction mechanism is controlled by the acid-catalyzed step [20] and therefore the formation of isopentane can be taken as an indirect measure of the activity of the acid function. It can be seen in Table 2 that the addition of Re to the monometallic Pt catalyst improved conversion, methane and propane formation and slightly modified the selectivity to *i*-C<sub>5</sub>. The superior conversion at the end of the run of the Pt–Re catalysts compared to Pt catalysts can be explained by taking into account the lower deactivation of the bimetallic catalyst. Moreover the higher methane formation can be attributed to the higher hydrogenolytic activity of the Pt–Re ensembles as shown in Table 1. The addition of indium to Pt–Re catalysts leads to a decrease in the conversion of *n*-pentane. This can be related to the acidity loss detected in the pyridine TPD tests. In the *n*-pentane reaction test the acid function can produce *i*-C<sub>5</sub> branched isomers through isomerization, light gases (C<sub>1</sub>–C<sub>3</sub>) through cracking and coke deposits through polymerization of the olefinic intermediates produced by the metal function. The acid strength necessary for cracking is greater than that needed for isomerization. For this reason the higher selectivity to *i*-C<sub>5</sub> of the In-doped catalysts in comparison to Pt–Re catalysts can be explained by the elimination of the sites of strong acidity. In this way the selectivity of the catalyst is modified and isomerization reactions are favored and cracking reactions are inhibited. The selectivity to *i*-C<sub>5</sub> is thus increased and the selectivity to C<sub>3</sub> is decreased after addition of indium.

The values of  $\chi = [(initial\ conversion - final\ conversion)/initial\ conversion]$  of the Pt–Re–In catalysts are also shown in Table 2. This parameter is related to the deactivation of the catalysts, being lower for the more stable catalysts. It may be that Re improves the stability of the Pt catalyst. On the other hand, the results indicate that the indium doped catalysts are more stable than the base Pt–Re ones. This can be explained by recalling that coke formation is a complex reaction in which on one side the metal

function produces the dehydrogenated intermediates [22] while on the other it destroys them with its hydrogenolytic activity [23]. The polymerization capacity of the dehydrogenated intermediates on the acid function is also important [11]. Then, the better stability of the Pt–Re catalysts is due to the fact that Pt–Re ensembles are more hydrogenolytic than Pt atoms (see Table 1) and they can destroy the coke precursors; as a consequence, the methane formation is increased. The lower coking rate of the catalysts doped with indium can be due to a lower acid strength leading to a higher catalyst stability. Finally, the results of Table 2 also indicate that addition of indium decreases the hydrogenolytic activity of the Pt–Re catalyst. This is in agreement with the CP hydrogenolysis results shown in Table 1.

Figure 3 shows the values of *n*-C<sub>7</sub> conversion as a function of time when using the PtReIn(*x*) catalysts. It can be seen that all the catalysts suffer deactivation by coke formation. At the beginning of the reaction (5 min) the three catalysts have practically the same activity. However at the end of the test, the catalyst with 0.3% In is the most active, followed by the 0.1% In catalyst. The higher deactivation suffered by the PtRe catalyst is attributed to its higher acidity and its greater capacity for forming dehydrogenated coke precursors. The lower deactivation of the PtReIn(0.3) correlates with its lower acidity.

Figure 4 shows that the addition of indium drastically decreases the formation of gases (C<sub>1</sub> + C<sub>2</sub> + C<sub>3</sub>). This occurs because the added indium interacts with the active metal phase (PtRe) and destroys the ensembles that are active in hydrogenolysis. Methane production is thus suppressed. In addition, the acidity of the support also decreases (Fig. 2) and in consequence, the cracking

**Table 2** Final values (at 240 min) of conversion and selectivity to certain products. *n*-pentane reaction

Catalyst	Conversion (%)	$(X_i - X_f)/X_i$	Selectivity (%)		
			<i>i</i> -C <sub>5</sub>	C <sub>1</sub>	C <sub>3</sub>
Pt <sup>a</sup>	32.2	0.63	20.2	0.8	4.7
Pt–Re	36.6	0.58	23.2	2.1	9.5
Pt–Re–In (0.1)	33.4	0.20	27.0	1.1	2.0
Pt–Re–In (0.3)	22.1	0.11	10.5	0.3	0.4

X<sub>*i*</sub>: conversion at 5 min TOS, X<sub>*f*</sub>: conversion at 240 TOS

<sup>a</sup> Pieck et al. [27]

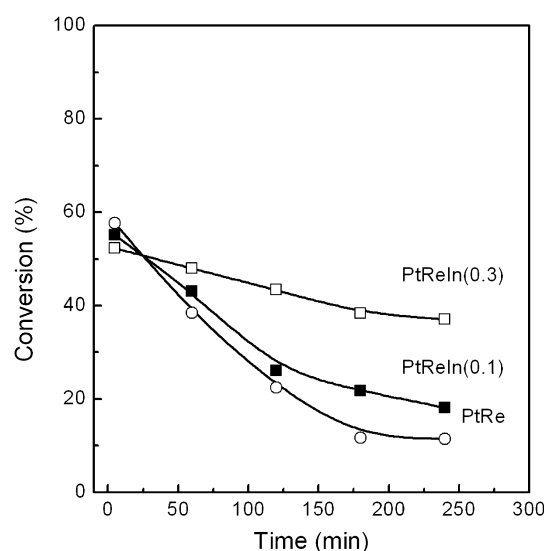


**Fig. 3** Conversion of *n*-C<sub>7</sub> as a function of time. In-free and In-doped catalysts

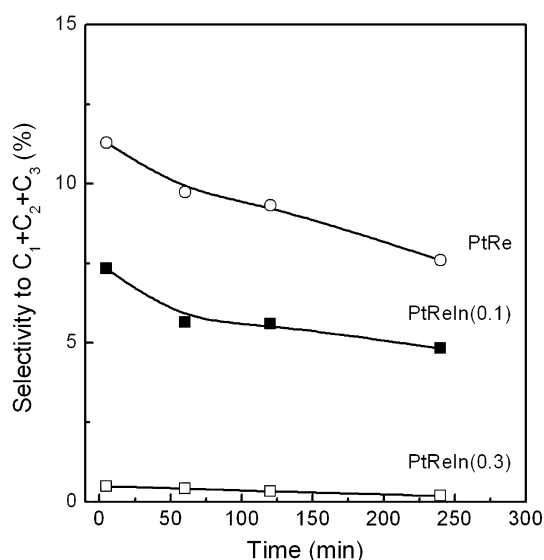


**Fig. 4** Selectivity to gases ( $C_1 + C_2 + C_3$ ) as a function of time. In-free and In-doped catalysts. *n*-heptane reaction

reactions (forming  $C_2$  and  $C_3$ ) that are controlled by the acid function are inhibited [24].

Table 3 shows the selectivity values of  $C_7$  isomers at 5 and 240 min of time-on-stream. PtRe has similar levels of activity for dehydrocyclization and isomerization because the values of selectivity to *i*- $C_7$  and aromatic hydrocarbons are similar. The addition of indium produces a marked change in the selectivity. The selectivity to aromatics is increased and the selectivity to  $C_7$  isomers is decreased. These results agree with similar ones reported by other authors [3, 5, 6] that point to an increase in the yield of aromatics upon the addition of indium to naphtha reforming catalysts.

The results can be explained by considering that the dehydrocyclization of *n*- $C_7$  leading to toluene is the result of the combination of both acid and metal-catalyzed elemental steps. The metal produces the dehydrogenation intermediates while the ring closure is performed on the acid sites. This last step is the rate controlling one [25].

During the reactions of isomerization of *n*- $C_5$  and reforming of *n*- $C_7$  coke is deposited over the catalyst. At the reaction conditions used (atmospheric pressure) coking is important and in a short time a great decrease of

**Table 3** Values of selectivity to aromatics and  $C_7$  isomers at 5 and 240 min of time-on-stream

Time (min)	Selectivity to aromatics (%)			Selectivity to <i>i</i> - $C_7$ (%)		
	PtRe	PtReIn0.1	PtReIn0.3	PtRe	PtReIn0.1	PtReIn0.3
5	18.9	69.90	44.74	15.9	6.19	1.02
240	4.40	46.15	31.67	6.70	2.20	0.10

the catalytic activity occurs. Temperature programmed oxidation (TPO) of the coke deposits formed enables to distinguish between the deposits formed on the metal sites and on the acid support. Two peaks or coke combustion zones can be distinguished. The coke that burns off at a low temperature corresponds to coke on metal sites while the coke that burns at high temperatures is located on acid sites [26]. Commonly the limit between the two combustion zones is located at 350–370 °C. TPO enables to assess the degree of polymerization of coke because the peak of combustion is shifted to higher temperatures as the degree of polymerization increases. Figure 5 shows the TPO traces of the carbon deposits formed on the PtRe and PtReIn catalysts at the end of the reaction of *n*- $C_5$  and *n*- $C_7$ . It can be seen that the coke on the PtRe catalyst after the *n*- $C_5$  reaction, has a combustion peak at about 460 °C that can be attributed to the burning of carbon on the support. At temperatures between 120 and 250 °C the combustion of coke on the metal would occur. When a third metal is added to the metal function a remarkable decrease of the coke content occurs. This is due to the fact that coking is a structure-sensitive reaction and that indium atoms decrease the effective size of Pt and Re ensembles thus inhibiting the formation of coke on the metal function. The TPO of the coke formed in the *n*- $C_7$  reforming reaction confirms that coke is preferentially deposited over the acid sites and is burned-off at a higher temperature than that formed in the

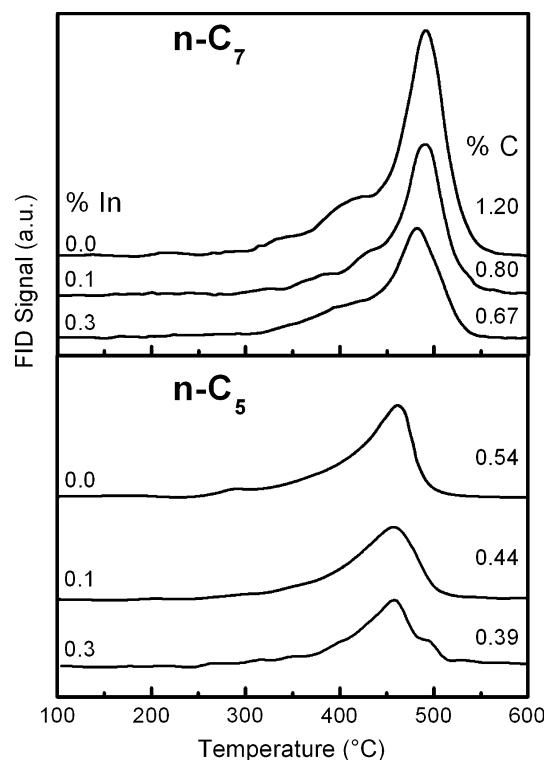


**Fig. 5** TPO traces of the In-free and In-doped catalysts

reaction of n-C<sub>5</sub>. The TPO of the Pt–Re catalyst run in n-C<sub>7</sub> shows a shoulder peak about 400 °C that could be due to the coke deposited on the support, in the vicinity of the metal. This phenomenon was previously observed by Duprez et al. [27]. They reported that this coke results from a continuous slow migration of carbonaceous fragments from the metal to the support.

The addition of Re to Pt generally leads to a decrease of the coking rate and an increase in the formation of light gases. Some authors conclude that the decrease of the coking rate is the result of the destruction of coke precursors by hydrogenolysis on metal sites [22]. In the case of the trimetallic catalysts the lower coking rate in comparison to the base catalyst is related to a lower formation rate of coke precursors. These are dehydrogenated, olefinic compounds that undergo polymerization on acid sites. The CH dehydrogenation tests showed that the addition of a third inactive metal (In) decreases the dehydrogenation activity of the PtRe catalyst. Another factor influencing the deposition of coke is the nature of the acid function. Sites of strong acidity are responsible for polymerization reactions leading to the formation and accumulation of coke. Therefore the lower coking rate in the In-doped catalysts can be attributed to the lower formation rate of coke precursors and to the lower acidity of the coking sites.

#### 4 Conclusions

The analysis of the TPR traces indicates the presence of indium species interacting with Re. The addition of indium to a Pt–Re/Al<sub>2</sub>O<sub>3</sub> catalyst produces a marked decrease in acidity, the effect being greater at increasing indium loading. It also causes an inhibition of the metal function properties, namely, dehydrogenation and hydrogenolysis.

The results of n-C<sub>5</sub> isomerization show that indium decreases the total activity of the Pt–Re catalyst. However the selectivity to pentane isomers is increased and the selectivity of low value light gases is decreased. The results of the reforming reaction of n-C<sub>7</sub> show that indium increases the stability and selectivity to aromatics, thus reducing the production of light gases and C<sub>7</sub> isomers. The

overall modifications of the Pt–Re base catalyst lead to a reduced formation of coke.

#### References

1. Klusksdahl HE (1968) US Patent 3,415,737
2. Baird WC, Boyle JP, Swan III GA (1992) US Patent 5,106,809
3. Bogdan PL, Imai T (2000) US Patent 6,048,449
4. Wilhelm FC (1976) US Patent 3,951,868
5. Antos GJ (1976) US Patent 4,032,587
6. Bogdan PL, Imai T (1999) US Patent 5,858,908
7. le Peltier F, Deves JM, Clause O, Kolenda F, Brunard N (2003) US Patent 6,511,593
8. Pieck CL, Vera CR, Querini CA, Parera JM (2005) Appl Catal A 278:173
9. de Miguel SR, Scelza OA, Castro AA (1988) Appl Catal 44:23
10. Perdigon-Melon JA, Gervasini A, Auroux A (2005) J Catal 234:421
11. Mazzieri VA, Grau JM, Vera CR, Yori JC, Parera JM, Pieck CL (2005) Catal Today 107:643
12. Carvalho LS, Pieck CL, Rangel MC, Fígoli NS, Vera CR, Parera JM (2004) Appl Catal A 269:105
13. Přebilová L, Dvořák B (2009) J Chromatography A 1216:4046
14. Selli E, Forni L (1999) Microporous Mesoporous Mater 31:129
15. Park PW, Ragle CS, Boyer CL, Balmer ML, Engelhard M, McCready D (2002) J Catal 210:97
16. Mazzieri VA, Grau JM, Yori JC, Vera CR, Pieck CL (2009) Appl Catal A 354:161
17. Gault FG (1981) Adv Catal 30:1
18. Boudart M, Aldag A, Benson JE, Dougharty VA, Harkings CG (1966) J Catal 6:92
19. Querini CA, Fígoli NS, Parera JM (1989) Appl Catal 52:249
20. Pieck CL, Marecot P, Parera JM, Barbier J (1995) Appl Catal A 126:153
21. Mazzieri VA, Grau JM, Vera CR, Yori JC, Parera JM, Pieck CL (2005) Catal Today 107–108:643
22. Barbier J (1987) In: Delmon B, Froment GF (eds) Catalyst deactivation. Elsevier, Amsterdam, p 1
23. Cooper BJ, Trinn DL (1980) In: Delmon B, Froment GF (eds) Catalyst deactivation. Elsevier, Amsterdam, p 63
24. Parera JM, Fígoli NS (1995) In: Antos GJ, Aitani AM, Parera JM (eds) Catalytic naphtha reforming: science and technology, Chap 3. Marcel Dekker, New York
25. Parera JM, Fígoli NS, Traffano EM, Beltramini JN, Martinelli EE (1983) Appl Catal 5:33
26. Pieck CL, Jablonski EL, Parera JM, Frety R, Lefebvre F (1992) Ind Eng Chem Res 31(4):1017
27. Duprez D, Hadj-Aissa M, Barbier J (1989) Appl Catal 49:67